

Monopole Oscillations and Dampings in Boson and Fermion Mixture in the Time-Dependent Gross-Pitaevskii and Vlasov Equations

Tomoyuki Maruyama,^{1,2,3,4} Hiroyuki Yabu,⁴ and Toru Suzuki⁴

¹ Institute for Nuclear Theory, University of Washington, Seattle, Washington 98195, USA

² College of Bioresource Sciences, Nihon University, Fujisawa 252-8510, Japan

³ Advanced Science Research Center, Japan Atomic Energy Research Institute, Tokai 319-1195, Japan

⁴ Department of Physics, Tokyo Metropolitan University,

1-1 Minamiohsawa, Hachioji, Tokyo 192-0397, Japan

(Dated: March 23, 2024)

We construct a dynamical model for the time evolution of the boson-fermion coexistence system. The dynamics of bosons and fermions are formulated with the time-dependent Gross-Pitaevsky equation and the Vlasov equation. We thus study the monopole oscillation in the boson-fermion mixture. We find that large damping exists for fermion oscillations in the mixed system even at zero temperature.

PACS numbers: 32.80.Pj, 67.57.Jj, 51.10.+y

I. INTRODUCTION

Over these last several years, there has been significant progress in the production of ultracold gases which realize the Bose-Einstein condensates (BECs) [1, 2, 3, 4], degenerate atomic Fermi gases [5], and Bose-Fermi mixtures [6]. These systems offer great promise for studies of new, interesting driven phenomena. One of the most exciting themes in recent physics is to study the time-dependent dynamical motion of trapped atoms, such as collective oscillations [2], quantum vortices [7] and atomic novae [8]. From a theoretical point of view, these phenomena are very important, as they allow us to construct and examine the transport theory in finite many-body systems. Many-body atomic systems are good probes for such study because the fundamental interactions are well understood and can be changed using the Feshbach resonance [9].

Of the above phenomena collective oscillations are very sensitive to properties of the system and therefore

e-mail: tomoo@brs.nihon-u.ac.jp

are condensates for studying time-dependent dynamics. The collective oscillation of BECs have been studied experimentally [10] and theoretically [11]. Furthermore, there have been theoretical studies of the Fermi gas in the normal phase [12] and in the superconducting phase [13], as well as the Bose-Fermi mixed gases [14, 15, 16, 17] and the BEC-BCS crossover [18].

Collective motions are usually studied with the random phase approximation (RPA). The RPA however, can only describe minimal vibrations around ground state; for example it is shown in Ref.[15] that the radial variation is only about 0.05 %, while the amplitudes of actual experimental can be as large as 10 %.

To describe collective oscillations with larger amplitudes we need to calculate the time evolution of the system using the time-dependent Gross-Pitaevsky (TDGP) and time-dependent Hartree Fock (TDHF) equations. In atomic gas systems, however, the fermion number is greater than one thousand, but it is not easy to solve the TDHF equations with so many fermions and limited computer resources. For system with large fermion number, on the other hand, the semi-classical approximation ($\hbar \rightarrow 0$) becomes useful, and the Vlasov equation, corresponding to the semi-classical approximation of the TDHF equations, can be used.

In nuclear physics [19] the Vlasov-Uhling-Uhlenbeck (VUU) approach, which is the Vlasov plus two body collision with the Pauli blocking, has been introduced, and very nicely explained many kinds of observables in heavy-ion collisions [20]. In addition, this approach has been developed for the Lorentz covariant framework including the non-local mean-fields [21]. As for the boson gas the time evolution of condensed bosons and thermal bosons have also been described with the time-dependent Gross-Pitaevsky equation and the Boltzmann equation [22]. Furthermore C. M. Enotti et al. [23] studied the expansion of a Fermi gas by calculating the Vlasov equation with the scaling method.

In this work we construct a transport model including the condensed bosons and fermions based on the TDGP and Vlasov equations. As a first step we study the collective monopole motion of a the spherically symmetric system at zero temperature. This calculation is a good test for the comparison between the RPA and direct time evolution calculations. In addition one pays attention to the monopole oscillation from the point of the view of the collapse so as to know compressing processes of systems [24].

In section 2, we describe our transport model. In Sec. 3 we give our results for monopole oscillations in the bose-fermi mixture, and discuss their properties. We then summarize in Sec. 4.

II. FORMALISM

Here we briefly explain our formalism. In this work we consider the spherical boson-fermion mixing gas at zero temperature.

First we define the Hamiltonian for boson-fermion coexistence systems as follows.

$$H = H_B + H_F + H \quad (1)$$

with

$$H_B = \int d^3x \left[\frac{1}{2} \dot{\psi}^2(x) r^2 + \frac{1}{2} x^2 \dot{\psi}^2(x) + \frac{g_B}{2} \psi^2(x) \dot{\psi}^2(x) \right]; \quad (2)$$

$$H_F = \int d^3x \left[\frac{1}{2m_f} \dot{\psi}^2(x) r^2 + \frac{1}{2} m_f \dot{\psi}^2(x) x^2 \right]; \quad (3)$$

$$H_{BF} = h_{BF} \int d^3x \dot{\psi}^2(x) \dot{\psi}^2(x); \quad (4)$$

where ψ and $\dot{\psi}$ are boson and fermion fields, respectively.

The fermion mass m_f and trapped frequency ω_f are normalized with the boson mass M_B and the boson trapped frequency ω_B , respectively. The coordinates are normalized by $r_B = (\hbar M_B \omega_B)^{1/2}$. The coupling constants g_B and h_{BF} are given as

$$g_B = 4 a_{BB}^{-1}; \quad (5)$$

$$h_{BF} = 2 a_{BF}^{-1} (1 + m_f^{-1}); \quad (6)$$

where a_{BB} and a_{BF} are the scattering lengths between two bosons and between the boson and the fermion, respectively.

In this work we only consider only zero-temperature, so that we can approximate the system with only the condensed bosons and degenerate fermions. Namely the total wave function is written as

$$\Psi(\mathbf{r}) = \prod_{i=1}^N \psi(\mathbf{r}_i) \phi(\mathbf{r}_i); \quad (7)$$

where ψ is the time normalized by r_B^{-1} , ϕ is a wave function of the condensed boson, and ϕ is a Slater determinant of fermions with single particle wave functions ϕ_n .

The time evolution of the wave functions are obtained from the variational condition that

$$\int d^3r \left[\frac{1}{2} \dot{\Psi}^2(\mathbf{r}) - H \Psi(\mathbf{r}) \right] = 0; \quad (8)$$

From this condition we derive coupled equations of the TDGP and TDHF equations as follows.

$$i\frac{\partial}{\partial t} \psi_c(\mathbf{x}; t) = \left[\frac{1}{2} \mathbf{r}^2 + U_B(\mathbf{x}) \right] \psi_c(\mathbf{x}; t); \quad (9)$$

$$i\frac{\partial}{\partial t} \psi_n(\mathbf{x}; t) = \left[\frac{1}{2m_f} \mathbf{r}^2 + U_F(\mathbf{x}) \right] \psi_n(\mathbf{x}; t) \quad (10)$$

with

$$U_B(\mathbf{x}) = \frac{1}{2} \mathbf{x}^2 + g_B \rho_B(\mathbf{x}) + h_{BF} \rho_F(\mathbf{x}); \quad (11)$$

$$U_F(\mathbf{x}) = \frac{1}{2} m_f \mathbf{x}^2 + h_{BF} \rho_B(\mathbf{x}); \quad (12)$$

where t is the time normalized by τ_B^{-1} and ρ_B and ρ_F are boson and fermion densities which are given as

$$\rho_B(\mathbf{x}) = N_B \int d\mathbf{p} |\psi_c(\mathbf{x}; \mathbf{p}; t)|^2; \quad (13)$$

$$\rho_F(\mathbf{x}) = \sum_n \int d\mathbf{p} |\psi_n(\mathbf{x}; \mathbf{p}; t)|^2; \quad (14)$$

The number of fermions are too large to solve the above TDHF equations directly, so instead one uses the semi-classical approach. In the semi-classical limit ($\hbar \rightarrow 0$) the TDHF equation is equivalent to the following Vlasov equation [25]:

$$\frac{d}{dt} f(\mathbf{x}; \mathbf{p}; t) = \left[\frac{\partial}{\partial t} + \frac{\mathbf{p}}{m_f} \cdot \nabla_{\mathbf{x}} - [\nabla_{\mathbf{x}} U_F(\mathbf{x})] \cdot \nabla_{\mathbf{p}} \right] f(\mathbf{x}; \mathbf{p}; t) = 0; \quad (15)$$

where $f(\mathbf{x}; \mathbf{p}; t)$ is the fermion phase-space distribution function defined as

$$f(\mathbf{x}; \mathbf{p}; t) = \int d^3z \delta\left(\mathbf{x} - \frac{1}{2}\mathbf{z}; t\right) \delta\left(\mathbf{p} - \frac{1}{2}\mathbf{z}; t\right) \psi(\mathbf{x}; \mathbf{p}; t) \psi^*(\mathbf{x}; \mathbf{p}; t); \quad (16)$$

As an actual numerical method we introduce the collective coordinate method and the test particle method [26] to solve the TDGP equation (9) and the Vlasov equation (15), respectively.

The wave function of the condensed boson ψ_c is expanded with the s-wave harmonic oscillator wave function $u_n(\mathbf{x})$ as

$$\psi_c(\mathbf{x}; t) = \sum_{n=0}^{N_{\text{base}}-1} A_n e^{i\phi_n} u_n(\mathbf{x}) e^{-\frac{1}{2} \mathbf{x}^2}; \quad (17)$$

where N_{base} is the number of the harmonic oscillator bases, and b , ϕ_n , A_n and ϕ_n are the time-dependent variables.

As for the fermion the phase-space distribution function is described as

$$f(\mathbf{x}; \mathbf{p}; t) = \frac{(2\pi)^3}{N_T} \sum_{i=1}^{N_T} \psi_i(\mathbf{x}; t) \psi_i^*(\mathbf{x}; t) \delta(\mathbf{p} - \mathbf{p}_i(t)); \quad (18)$$

where N_T is number of test-particles per fermion.

Then we define the Lagrangian with these coordinates as

$$L(A_n; b; x_i; p_i) = N_B \int d^3x \left[\frac{1}{2} \dot{c}^2(x) + \frac{1}{N_T} \sum_{i=1}^X p_i \frac{d}{dt} x_i \right] - E_T; \quad (19)$$

with the total energy E_T written as

$$E_T = \langle H \rangle = E_B + E_F + E_{BF}; \quad (20)$$

and

$$E_B = \int d^3x \left[\frac{1}{2} \dot{c}^2(x) + \frac{g_B}{2} c^2(x) \right]; \quad (21)$$

$$E_F = \frac{1}{N_T} \sum_{i=1}^X \left[\frac{1}{2m_f} p_i^2 + \frac{1}{2} m_f \dot{x}_i^2 \right]; \quad (22)$$

$$E_{BF} = \frac{1}{N_T} \sum_{i=1}^X h_{BF}(x_i); \quad (23)$$

In the above equations we take $A_n; b;$ and $x_i; p_i$ as time-dependent variables.

The time evolution of these variables are given by the Euler-Lagrange equations with respect to the time-dependent variables. For example, the Euler-Lagrange equations for the fermions with respect to x_i and p_i , become the following classical eq. of motion for the test particles,

$$\frac{d}{dt} x_i(t) = \frac{p_i}{m_f}; \quad (24)$$

$$\frac{d}{dt} p_i(t) = -\nabla U(x); \quad (25)$$

We can also obtain the same equations by substituting eq.(18) into eq.(15). Note here that the test-particle motion describes the time evolution of the fermion gas, and does not correspond to actual single particle motion.

III. RESULTS

In this section we show the results of our calculation on the monopole oscillation in the boson-fermion mixture. In order to know the characteristic behavior of the boson-fermion mixed system, we consider only the system where the boson number N_b is much larger than the fermion number N_f ($N_b \gg N_f$), which optimizes the overlap of bosons and fermions. This is because the condensed boson density tends to be located in the central region while the fermion density distributes over a large region due to Pauli blocking.

In this work we deal with the system $^{39}\text{K}-^{40}\text{K}$, where the number of the bosons (^{39}K) and the fermions (^{40}K) are $N_b = 100000$ and $N_f = 1000$. The mass difference between the two atoms is omitted, $m_f = 1$. The trapped frequencies are taken as $\omega_B = 100$ (Hz) and $\omega_f = 1$. The boson-boson interaction parameter g_B is taken to be $g_B = 1.34 \times 10^2$, which corresponds to $a_{BB} = 4.22$ (nm) [27]; in addition we vary the boson-fermion interaction parameter h_{BF} which is measured in units of $\hbar_0 = 7.82 \times 10^3$ corresponding to $a_{BF} = 2.51$ (nm) [27]. In the numerical calculation we take the number of the harmonic oscillator bases for the condensed boson to be $N_{\text{base}} = 11$ and the number of the test-particle per fermion to be $N = 100$.

A . Ground State

Before performing the numerical calculation of collective motion, we explain the method to construct the ground state under the above formalism. The ground state is defined as the stationary state with the lowest energy.

In the stationary condition the wave function of the condensed boson satisfies $\partial_t \psi = 0$, and $\partial E_T / \partial b = \partial E_T / \partial A_i = 0$. We can obtain the wave function of the condensed bosons by repeating the processes of solving these stationary conditions and diagonalizing the Hamiltonian matrix with the base of the harmonic oscillator wave functions.

The fermion phase-space distribution function is given by the Thomas-Fermi approximation,

$$f(\mathbf{x}; \mathbf{p}) = \left[\frac{1}{2\pi\hbar} \right]^3 \exp[-\beta U_F(\mathbf{x}; \mathbf{p})] \quad (26)$$

with

$$U_F(\mathbf{x}; \mathbf{p}) = \frac{1}{2m_f} p^2 + U_B(\mathbf{x}) \quad (27)$$

Here we iterate solving the boson wave function and varying the fermi energy ϵ_f to give the correct fermion number.

For numerical simulations we distribute the test-particles to reproduce the phase-space distribution solved in the Thomas-Fermi approximation. In this process we have to insure the stability of the ground state.

In Fig. 1a we show the density distributions of the bosons and the fermions (multiplied one hundred) with the long-dashed and dashed lines, respectively. We take the boson-fermion coupling to be $h_{BF} = \hbar_0$. We see a large overlap region between boson and fermion densities. In addition we show test-particle

distribution with $N_T = 100$ in Fig. 1b, where the histogram indicates the test-particle distribution while the dashed line denotes the density in the Thomas-Fermi approximation. We see that the two results very nicely agree.

As a next step we examine the stability of the ground state by performing a time evolution starting from above the ground state. In Fig. 2 we show the time dependence of the root-mean-square-radius (RMSR) for the bosons (R_b) and the fermions (R_f) with long-dashed and dashed lines, respectively. These results show that their RMSRs vary only within 0.01 % over the entire time-evolution, and confirm that the ground state is very stable. Hence we can get very stable and reasonable ground states for the dynamical calculations.

B. Monopole Oscillations

In this subsection we show our calculational results for the monopole oscillations. We take the boson-fermion coupling to be $h_{BF} = h_0$ in all calculations in this subsection.

At the beginning of the numerical simulations we scale the boson wave function ψ_b and the fermion phase-space distribution function from those in the ground state as follows. By using the scaling parameter s_b and s_f , we scale the boson parameter b and the position (x_i) and momentum (p_i) coordinates of the i -th fermions as

$$b(0) = b^{(g)} = \frac{b^{(g)}}{s_b}; \quad (28)$$

$$x_i(0) = s_f x_i^{(g)}; \quad p_i(0) = p_i^{(g)} s_f; \quad (29)$$

where superscripts (g) represent the coordinates in the ground state. Then we perform the numerical calculation of the monopole oscillations with various initial conditions.

In order to see appearance of the monopole oscillation, we define

$$x_i(t) - R_i(t) = R_i^0 - 1 \quad (i = B, F); \quad (30)$$

where $R_B(t)$ and $R_F(t)$ are the RMSRs of the bosons and fermions at time t , and R_B^0 and R_F^0 are the RMSRs in the ground state obtained by the Thomas-Fermi approximation.

In Fig. 3 we show the time-dependence of x_B (a) and x_F (b) with the initial conditions $x_B(0) = 0.1$ ($s_b = 1.1$) and $x_F(0) = 0.1$ ($s_f = 1.1$) (in-phase). In addition we exhibit results with other initial conditions: $x_B(0) = 0.1$ ($s_b = 1.1$) and $x_F(0) = -0.1$ ($s_f = 0.9$) (out-of-phase) in Fig. 3b, $x_B(0) =$

0.1 ($s_b = 1.1$) and $x_F(0) = 0$ ($s_f = 1.0$) in Fig. 3d. The condensed bosons oscillate independently of the fermions, so that the difference between x_B at these three initial conditions is not visible.

In the above three cases we see that the fermion oscillations are forced vibrations with a beat, which gradually becomes blurred. This blurring cannot be explained within the RPA.

Before discussing this blurring we calculate with another initial condition: $x_B(0) = 0$ ($s_b = 1.0$) and $x_F(0) = 0.1$ ($s_f = 1.1$). With this initial condition the boson oscillation is weak and does not strongly affect the fermion oscillation, see Fig. 4. The boson oscillation has a beat which appears in early time and blurs in latter time stages, and the fermion oscillation has a strong damping. In Fig. 4c we show the results of the calculation at the same initial condition, but with the boson motion frozen; namely the fermions move in the fixed potential $U_F(x)$ in the ground state. The damping behavior of the fermion oscillation is almost the same as that in Fig. 4b, except that the fermion oscillation is monotonously damped while the oscillation in Fig. 4b undergoes one beat.

This damping process causes the blurring beat in the fermion oscillation shown in Fig. 3. Hence this damping process must play a significant role in collective motions in the boson-fermion mixtures. Next we inspect the origin of the damping by focusing on monopole motions with the initial condition $x_B(0) = 0$. Here we examine the time-evolution of the energy levels. In Fig. 5 we show the time-dependence of E_B (long-dashed), $E_F + E_{BF}$ (dashed) and E_{BF} (solid), which are defined in eqs. (20–23). Note that $E_F + E_{BF}$ corresponds to the sum of the fermion single particle energy.

First we note that the boson-fermion interaction part, E_{BF} , is much smaller than the boson part, E_B , and the fermion part, E_F . Second the boson part E_B and the fermion part, $E_F + E_{BF}$, do not significantly vary in the time-evolution process. After the damping ($\tau > 100$) the energies, normalized by $\sim \epsilon_B$, are given as

$$E_B = 7.04 \times 10^5 \quad (7.04 \times 10^5); \quad (31)$$

$$E_F + E_{BF} = 1.57 \times 10^4 \quad (1.54 \times 10^4); \quad (32)$$

$$E_{BF} = 1.54 \times 10^3 \quad (1.57 \times 10^3); \quad (33)$$

where the values in the brackets indicate the energy contribution to the ground state. The excited energy of the fermions is about 300 ($\sim \epsilon_B$) while the energy transfer is about 70 ($\sim \epsilon_B$) through the boson-fermion interaction. This fact implies that the damping is not caused by the fermion energy loss, and in addition that this oscillation state is a many-particle many-hole state because the excited energy of the one-particle

and one-hole states is about $2\sim \omega_B$ in the monopole oscillations.

Further we calculate the spectrum which is obtained by the Fourier transformation

$$F(\omega) = \int_{T_i}^{T_f} dt R^2(\omega) e^{i\omega t} \quad (34)$$

In order to discuss the oscillations, we vary T_i and T_f .

In Fig. 6 we show the results of the spectra obtained by integrating over the regions $0 < t < 80$ (damping period) for the bosons (a) and fermions (b), and over $100 < t < 200$ (after damping) for the bosons (c) and fermions (d). In addition we plot the spectra for fermion oscillation with the boson motion frozen, with the dashed lines in Fig. 6b and 6d.

In Fig. 6b we see that the peak position for the fermion spectrum is $\omega_M^f = 1.91$, and does not vary in any of the time regions while the width becomes slightly narrower after the damping is finished (Fig. 6d).

On the other hand there are two peaks for the boson spectra; at the frequency $\omega_M^b = 1.91$ and 2.23 in the fermion damping process. After the damping, there is only one boson oscillation mode at $\omega_M^b = 2.23$, similar to the fermion oscillation.

We can consider the intrinsic frequencies of the boson and fermion oscillations to be $\omega_M^b = 2.23$ and $\omega_M^f = 1.91$ in our calculation. The boson intrinsic frequency agrees with $\omega_M^b = \sqrt{\frac{P}{5}}$ which has been shown in the system only including the condensed bosons [2]. The boson intrinsic mode is almost independent of fermions because the boson number is much larger than the fermion number. In addition the frequency of the fermion oscillation is the same with or without the boson motion.

In the short time period both the boson and fermion oscillations can be approximately described within the linear response theory as

$$x_B = A_{bb} \cos(\omega_M^b t) + A_{bf} \cos(\omega_M^f t); \quad (35)$$

$$x_F = A_{fb} \cos(\omega_M^b t) + A_{ff} \cos(\omega_M^f t); \quad (36)$$

If the amplitude of the boson oscillation in the initial condition is not small, the boson oscillation negligibly involves a mode with the fermion intrinsic frequency, $A_{bb} \rightarrow A_{bf}$, and the fermion oscillation becomes the usual forced oscillation $A_{fb} \rightarrow A_{ff}$ as shown in Fig. 3.

When $x_B(0) = 0$ such as in Fig. 4, the fermion oscillation does not have a mode with the boson frequency ($A_{fb} \rightarrow 0$). In the beginnings these fermion oscillations trigger the boson oscillations, and then the boson oscillations dominantly hold the mode with the fermion frequency, $A_{bb} \rightarrow A_{bf}$. As the time evolves, the

amplitude of the boson oscillation becomes larger, but the amplitude of the fermion oscillation contrarily decreases, and the A_{bf} is gradually reduced by the damping of the fermion oscillation. The amplitude of the fermion oscillation becomes too small to influence the boson oscillation, the boson oscillation loses the mode with the fermion frequency, and its beat finally disappears.

The behavior of the fermion oscillation in the full calculation is the same as that when the boson motion is frozen, and the fermions do not lose energy through oscillation. Hence the fermions move almost independently each of other, and the damping of the fermion oscillations must come from properties of the fermion single particle motion.

The boson density is distributed in a smaller region than the fermion density, so the fermion potential does not have simple harmonic oscillator shape, which is shown with the solid line in Fig. 7. The Thomas-Fermi approximation, which is available in the case of the large boson number, gives the boson density as $\rho_B = (2\mu_B - x^2)/2g_B$, where μ_B is the boson chemical potential. Then the fermion potential U_F is approximately written as

$$U_F(x) \begin{cases} \approx \frac{\hbar_{BF}}{g_B} \rho_B + \frac{1}{2} (m_f \hbar_f^2 - \frac{\hbar_{BF}}{g_B}) x^2 & (|x| < \sqrt{\frac{\mu_B}{2g_B}}) \\ \approx \frac{1}{2} m_f \hbar_f^2 x^2 & (|x| > \sqrt{\frac{\mu_B}{2g_B}}) \end{cases} \quad (37)$$

Thus the fermion potential is separated into two region, the inside and outside of the boson populated region.

In the single harmonic oscillator potential the fermion motion is always harmonic in both the semi-classical and quantum approaches, but the above fermion potential, which is separated into the two regions, leads to anharmonicity when fermions move in the both regions.

In the quantum calculation this damping is explained with the phase factor of the fermion single particle wave functions given by their single particle energies. If the boson motion is frozen, the wave-function of the n -th fermion is written as

$$\psi_n(x; \mu) = \sum_i a_i^{(n)} v_i(x) e^{i\epsilon_i \mu} \quad (38)$$

where v_i is the wave-function of the i -th orbit of the ground state, ϵ_i is its single particle energy, and $a_i^{(n)}$ is a coefficient. The expectation value of x^2 is

$$\langle x^2 \rangle_n = \sum_i \int dx \psi_n^*(x; \mu) x^2 \psi_n(x; \mu) = \sum_{i,j} C_{ij} e^{i(\epsilon_j - \epsilon_i) \mu} \quad (39)$$

with

$$C_{ij} = \sum_n a_i^{(n)} a_j^{(n)} \int d^3x v_j(\mathbf{x}) x^2 v_i(\mathbf{x}) : \quad (40)$$

This coefficient is usually negligible when $j_i = j_j = 2$, and then

$$\langle x^2 \rangle = \sum_i \left[C_{i,i+1} + C_{i,i+1} e^{i(\omega_{i+1} - \omega_i)} + C_{i+1,i} e^{-i(\omega_{i+1} - \omega_i)} \right] : \quad (41)$$

When the fermion potential is only the harmonic oscillator potential, $\omega_{i+1} - \omega_i = 2\omega_f$, and the oscillation of $\langle x^2 \rangle$ does not exhibit a damping. As shown before, however, the fermion potential includes two kinds of harmonic oscillator potentials with the different frequency. In addition the potential in the boson region is not exactly that of the harmonic oscillator. Then the difference of the single particle energies, $\omega_{i+1} - \omega_i$, has dependence on i , and the fermion monopole oscillation includes various vibration modes with different frequencies, and its oscillation shows a damping. It was shown in Ref. [28] that an oscillation of population difference in two-component fermi gas has a damping because of a similar multimode dephasing.

In the semi-classical calculation, the frequencies of modes including the oscillation is continuous, though they are discrete in the full quantum calculation. In the system with large particle number, however, the semi-classical calculation well describes the time evolution of the phase space distribution. In the harmonic oscillator potential, especially, this time evolution completely agrees with that in the quantum calculation because higher order terms with respect to \hbar [25], which are omitted in eq.(15), exactly vanish. Hence our calculations sufficiently describe the actual time-evolution in the mean-field level.

In numerical simulations such oscillation properties are described by motions of the test-particles. A test particle passes over both regions, inside and outside of the boson region. Here we consider oscillation behavior of radial distance of this i -th test particles as $x_i(t)$. In a non-harmonic oscillator potential the period between successive maximum $x_i(t)$ depends on the orbit. This anharmonicity gradually reduces the amplitude of x .

As mentioned before, the amplitude is about $x \sim 10^{-4}$ in the RPA calculation and the excited energy is about $2\omega_B$. In the present calculation, however, the excited energy when $x_F(0) = 0.1$ ($s_F = 1.1$) is about $300\omega_B$. Oscillation states such as those in the present calculation are multiparticle and multi-hole states. Under an anharmonic potential, all test-particles do not oscillate with the same period, and hence this anharmonicity is the cause of the observed damping of x_F .

C . A m p l i t u d e a n d B o s o n - F e r m i o n C o u p l i n g D e p e n d e n c e s

In this subsection we investigate the oscillation behavior by changing the initial amplitude of fermion oscillation, $x_F(0)$, and the boson-fermion couplings, h_{BF} .

First we examine the amplitude dependence of the damping. In Fig. 8 we show the results with the initial conditions that $x_B(0) = 0$ and $x_F(0) = 0.01$ (small amplitude). The excited energy of this oscillation is about $30 (\sim \epsilon_B)$, which is still much larger than the one-particle one-hole excited energy. The strong damping also appears there even with such small amplitude oscillation, which becomes about 10^{-3} after the damping. The test particle method cannot however give sufficient accuracy to exactly describe oscillations with such small amplitudes after the damping. Therefore, the more detailed study lies beyond the scope of this work.

In Fig. 9 we show the results with the initial conditions that $x_B(0) = 0$ and $x_F(0) = 1.0$ (large amplitude); we do not see such strong damping though the excitation energy is about $1800 (\sim \epsilon_B)$. In Fig. 10 we show the spectra of the above boson and fermion oscillations for the large amplitude. The boson and fermion spectra have peaks at quite different frequencies. The boson spectrum has a large peak at the boson intrinsic frequency $\omega_M^f(a)$, while the fermion one has a peak at $\omega^f(b)$, which is the frequency of the monopole oscillation with only one harmonic oscillator potential. In the large amplitude oscillation most of the fermions have large kinetic energy in the central region and pass through this region quickly, so that the fermions mostly stay outside the boson density region. In large amplitude oscillations, therefore, the oscillation frequency agree with that only in the trapped potential and, the rapid damping does not appear. The final amplitude after the damping must be much larger than that when $x_F(0) = 0.01$.

Next we vary the strength of the boson-fermion coupling h_{BF} , and perform calculations of the oscillation at the same initial condition $x_B(0) = 0$ and $x_F(0) = 0.01$. We show the results with $h_{BF} = h_0 = 2$ in Fig. 11 and $h_{BF} = h_0 = 1$ in Fig. 12.

In Fig. 11 the features of the oscillation which have been seen in Fig. 4 are more clear; the damping of the fermion oscillation and the blur of the beat in the boson oscillation occurs sooner with $h_{BF} = 2h_0$ than $h_{BF} = h_0$.

If the boson-fermion coupling is negative, the oscillation behavior is a little different. When $h_{BF} = -h_0$ in Fig. 12, the fermion oscillation undergoes beating even after the motion is damped. Additionally

the amplitude of the boson oscillation is much larger than that of $h_{BF} > 0$. This beat of the fermion oscillation after the damping is caused by the rather large amplitude of the boson oscillation.

As the repulsive interaction between bosons and fermions is increased, the damping of the fermion oscillation is faster, but the amplitude of the boson oscillations do not increase. In the attractive interaction, however, the damping is still rapid, but the amplitude of the boson oscillation is large. We believe this difference comes from the overlap region between boson and fermion densities.

When the fermions feel a repulsive force in the boson density region (see Fig. 7), the fermions stay outside of this boson region and have little influence on the boson oscillation. Then the amplitude of the boson oscillation does not become larger, and its beat becomes blurred soon in spite of the stronger interaction.

When the interaction is attractive, on the other hand, many fermions move inside of the boson density region, and then boson and fermion motions are more significantly coupled.

IV . SUMMARY

In this paper we study the collective monopole oscillation of bose-fermion mixtures, where the number of bosons is much larger than that of fermions, by solving directly the time-dependent equations. When the initial amplitude is about 10 % of the ground state RMSR, we find a rapid damping of the fermion oscillation and a beat in the bosonic vibration at the early time stage while this damping and beat almost disappear in the later time stage. This rapid damping does not exist at zero temperature in the system including only one kind of boson [29]; it is a typical feature in the bose-fermion mixtures.

Our analysis shows this damping is caused by the anharmonicity of the multiparticle and multi-hole states. Since the fermion mean-field is separated into two parts, inside and outside of the boson density region, fermions feel very different forces in these two regions and their motions are not harmonic. Then these motions become chaotic, and the oscillation amplitude decreases.

In this work we focus on the oscillation with the initial condition $x_B(0) = 0$, where only the fermions have initial motion at the beginning. In this case we can clearly see damping properties of the fermion oscillation because the boson oscillation has very small amplitude. Even if the amplitude of the initial boson oscillation is larger, the damping also plays a significant role. When the fermion oscillations have a large amplitude, it always tends to cause damping, but the amplitude after the damping is enhanced, again, by the boson oscillation. The fermion oscillation repeats the damping and enhancement, and its

beat gradually blurs; the oscillation behavior is not recursive.

This damping process cannot be described with RPA, where the motion is assumed to be harmonic. As shown in Ref.[15] the excitation energy obtained in RPA corresponds to oscillations with the amplitude of 10^{-4} of RMSR. In actual experiments, however, the amplitude is not so small, the oscillation states are multiparticle and multi-hole states, and hence we must solve the time-dependent process directly. Even if the boson-fermion interactions are attractive, both the boson and fermion oscillations have an oscillation behavior similar to those in the repulsive interaction in the damping time stage. In the attractive interaction, however, the amplitude of the boson oscillation slightly increases and the fermion oscillation has a small beat after the damping time stage.

In this work we do not show calculations with stronger attractive force between bosons and fermions. If the attractive force is stronger, the frequency of the fermion oscillation becomes larger, and finally agrees with that of the boson intrinsic oscillation; where the two oscillation must make a resonance. We have investigated this phenomena, and found resonances which have quite different behaviors [30].

Furthermore we do not take into account two body collisions and thermal bosons. Since two fermions do not directly interact, dissipation of fermions occurs through collisions between fermions and thermal bosons. In the system $N_b \ll N_f$ at zero temperature, however, the thermal bosons are very few, and then the damping process shown in this work must be dominant in the early time stage. After this damping the collisional damping may play a role in the time-evolution process. In future we would like to introduce this collisional process in our simulation.

Acknowledgement

We thank Andre Walker-Laud for helpful comments on the manuscript. T.M. thanks the Institute for Nuclear Theory at University of Washington for the hospitality and partially support during the completion of this work.

[1] E.A. Comell and C.E. Wieman, Rev. Mod. Phys. 74, 875 (2002);

W. Ketterle, Rev. Mod. Phys. 74, 1131 (2002).

[2] F. Dalfovo, et al., Rev. Mod. Phys. 71, 463 (1999).

[3] C.J. Pethick and H. Smith, "Bose-Einstein Condensation in Dilute Gases", Cambridge University Press (2002).

[4] J.O. Andersen, Rev. Mod. Phys. 76, 599 (2004).

- [5] B. DeMarco and D. S. Jin, *Science* 285, 1703 (1999);
S. R. Granade, et al, *Phys. Rev. Lett.* 88, 120405 (2002).
- [6] A. G. Tuscott, K. E. Strecker, W. I. McA Alexander, G. B. Partridge, and R. G. Hulet, *Science* 291, 2570 (2001);
F. Schreck, et al, *Phys. Rev. Lett.* 87, 080403 (2001);
Z. Hadzibabic, et al, *Phys. Rev. Lett.* 88, 160401 (2002); 91, 160401 (2003).
- [7] M. R. Matthews, et al, *Phys. Rev. Lett.* 83, 2498 (1999).
- [8] J. L. Roberts, et al, *Phys. Rev. Lett.* 86, 4211 (2001).
- [9] H. Feshbach, *Ann. Phys. (NY)* 19, 287 (1962).
- [10] D. S. Jin, J. R. Ensher, M. R. Matthews, C. E. Wieman and E. A. Cornell, *Phys. Rev. Lett.* 77, 420 (1996);
M. O. Oewes et al, *Phys. Rev. Lett.* 77, 998 (1996).
- [11] T. Kinura, H. Saito and M. Ueda, *J. Phys. Soc. Jpn.* 68 (1999);
R. Graham and D. Walls, *Phys. Rev. A* 57, 484 (1998);
D. G. Gordon and C. M. Savage, *Phys. Rev.* 85, 1440 (1999).
- [12] G. M. Bruun, *Phys. Rev. A* 63, 043408 (2001);
K. Goral, M. W. Brewczyk and K. Rzewski, *Phys. Rev. A* 67, 025601 (2003).
- [13] G. M. Bruun and B. R. Mottelson, *Phys. Rev. Lett.* 87, 27403 (2001); G. M. Bruun and L. Viverite, *Phys. Rev. A* 64, 063606 (2001).
- [14] T. Miyakawa, K. Oda, T. Suzuki and H. Yabu, *J. Phys. Soc. Jpn.* 69, 2779 (2000).
- [15] T. Sogo, T. Miyakawa, T. Suzuki and H. Yabu, *Phys. Rev. A* 66, 013618 (2003);
T. Sogo, T. Suzuki and H. Yabu, *Phys. Rev. A* 68, 063607 (2003).
- [16] P. Capuzzi and E. S. Hernandez, *Phys. Rev. A* 64, 043607 (2001).
- [17] H. Pu, W. Zhang, M. W. J. Wilkens and P. M. Eystre, *Phys. Rev. Lett.* A 88, 070408 (2002).
- [18] H. Heidelberg, *Phys. Rev. Lett.* A 93, 040402 (2004).
- [19] G. F. Bertsch and S. DasGupta, *Phys. Rep.* 160 (1988) 189.
- [20] For example, W. Cassing and U. Mosel, *Prog. Part. Nucl. Phys.* 25 1990 235, and reference therein.
- [21] T. Manuyama, W. Cassing, U. Mosel, K. Weber, *Nucl. Phys. A* 573, 653 (1994).
- [22] B. Jackson and E. Zaremba, *Phys. Rev. A* 66, 033606 (2003).
- [23] C. Menotti, P. Pedri and S. Stringari, *Phys. Rev. Lett.* 89, 2450402-1 (2002).
- [24] M. Bartenstein, A. Altmeyer, S. Riedel, S. Jochim, C. Chin, J. H. Denschlag and R. Grimm, *Phys. Rev. Lett.* 92, 203201 (2004).
- [25] L. P. Kadanoff and G. Baym, "Quantum Statistical Mechanics" (1962), New York.
- [26] R. W. Hockney AND J. W. Eastwood, "Computer simulations using particles", McGraw-Hill, New York, 1981;
C. Y. Wong, *Phys. Rev. C* 25, 1460 (1982).

- [27] T. Miyakawa, et al, J. Phys. Soc. Japan, Vol. 69 (2000) 2779.
- [28] S. Poetting et al, Phys. Rev. A 65,063620 (2002); C. Search et al, Phys. Rev. Lett. 88, 110401 (2002).
- [29] F. Chevy, Phys. Rev. Lett. 88, 250402 (2002).
- [30] T. Manuyama, H. Yabu and T. Suzuki, Laser. Phys. Vol. 15 in press (cond-mat/0412494).

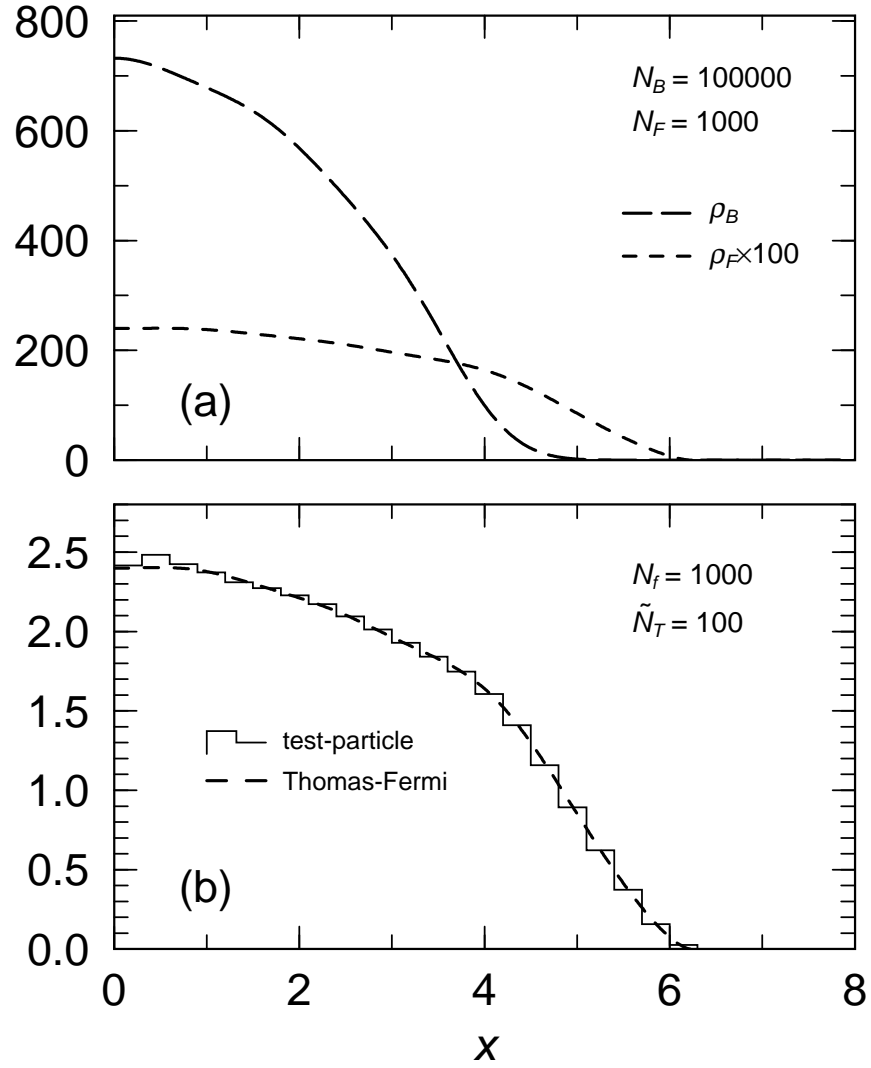


FIG. 1: The density-distribution of ground state of the boson (K^{39}) and fermion (K^{40}) mixed system with $h_{BF} = h_0$. The results of $N_B = 10000$ and $N_F = 1000$ are shown in Fig. 1a. The dimensionless distance x is in units of λ_B . The long-dashed and dashed lines indicate the densities of boson and fermion, respectively. In lower column the histogram show the results of the test particle.

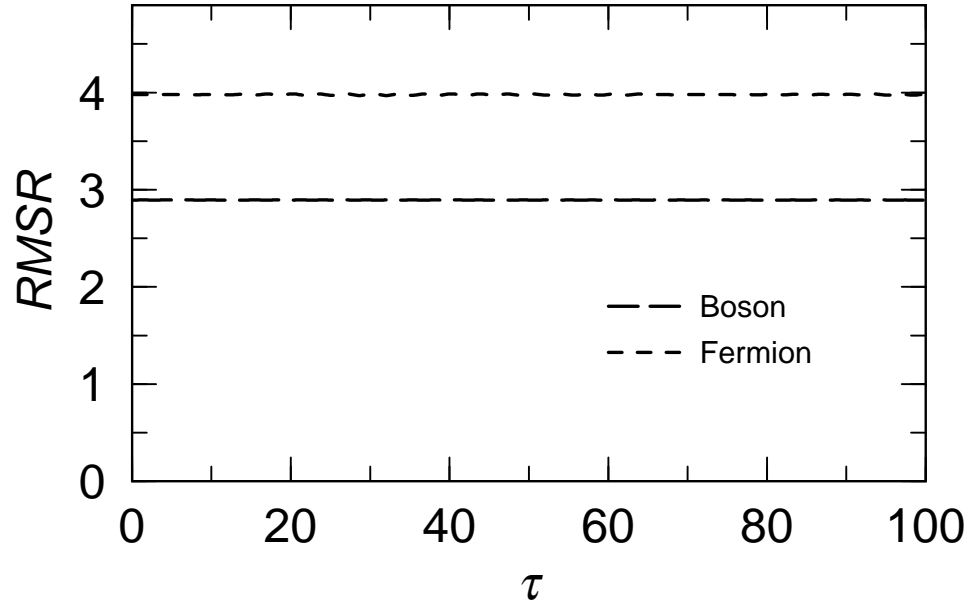


FIG. 2: The time-dependence of the root-mean-square radii normalized by r_B for $N_B = 100000$ and $N_F = 1000$ with $h_{B/F} = h_0$. The dimensionless time τ is in units of r_B^{-1} . The long-dashed and dashed lines indicate the boson and fermion root-mean-square radii (RMSR), respectively.

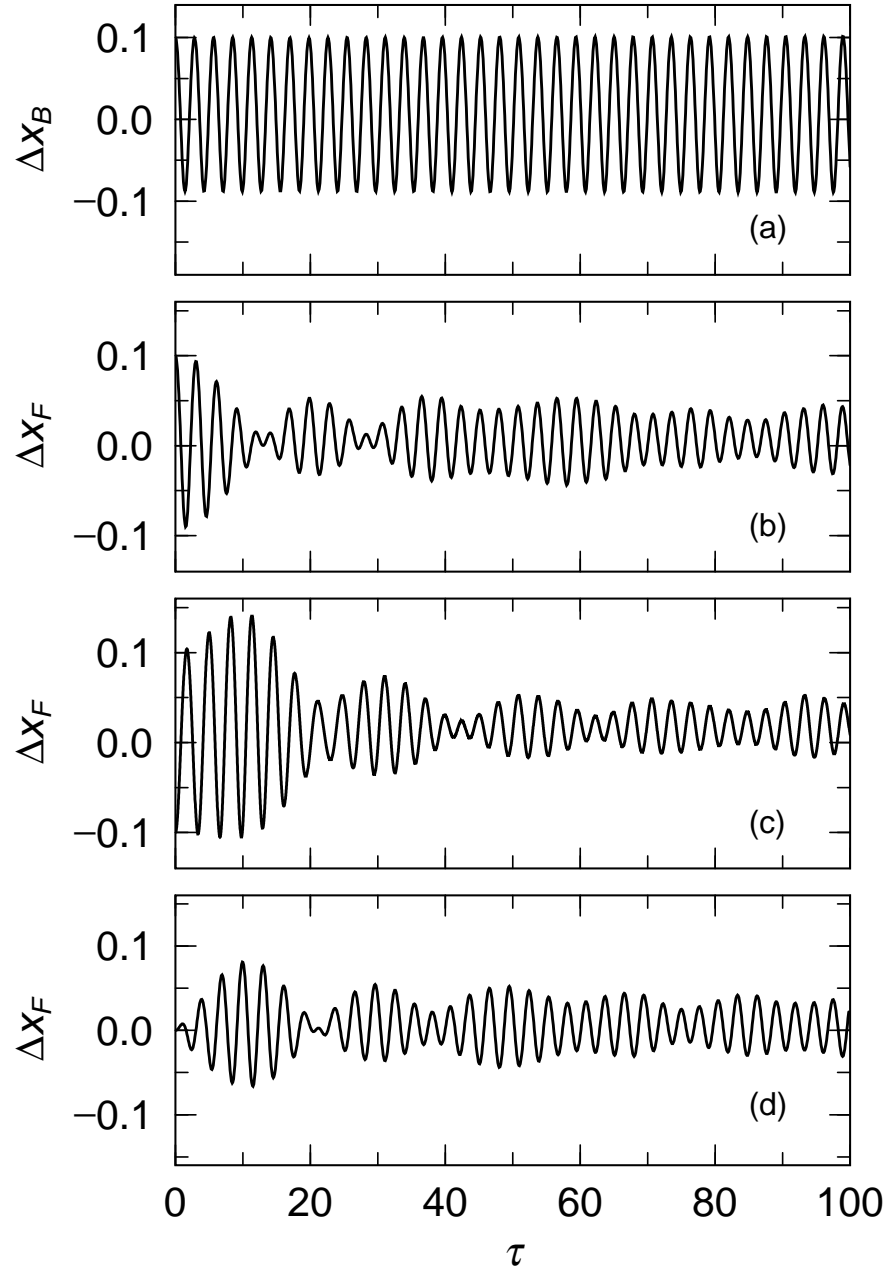


FIG. 3: Time evolution of x_B (a) and x_F (b) with $h_{BF} = h_0$ at the initial condition that $x_B(0) = 0.1$ and $x_F(0) = 0.1$. Time evolution of x_F at the initial conditions that $s_b = 1.1$ and $x_F(0) = 0.1$ (c), and $x_F(0) = 0$ (d).

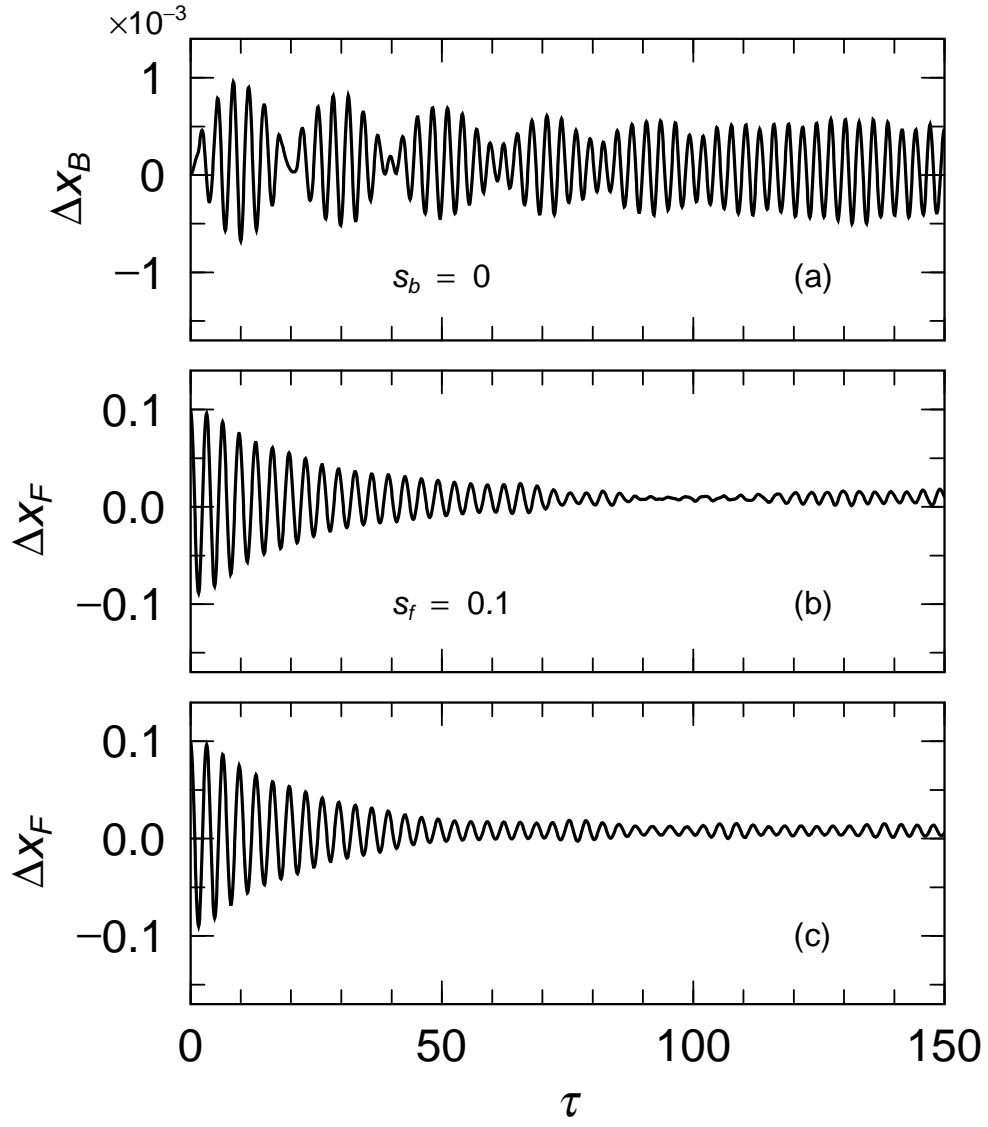


FIG. 4: Time evolution of x for boson (a) and fermion (b) with $h_{BF} = h_0$ at the initial condition that $x_B(0) = 0$ and $x_F(0) = 0.1$. In the last column time evolution of x for fermion (c) with freezing the boson motion at the same initial condition.

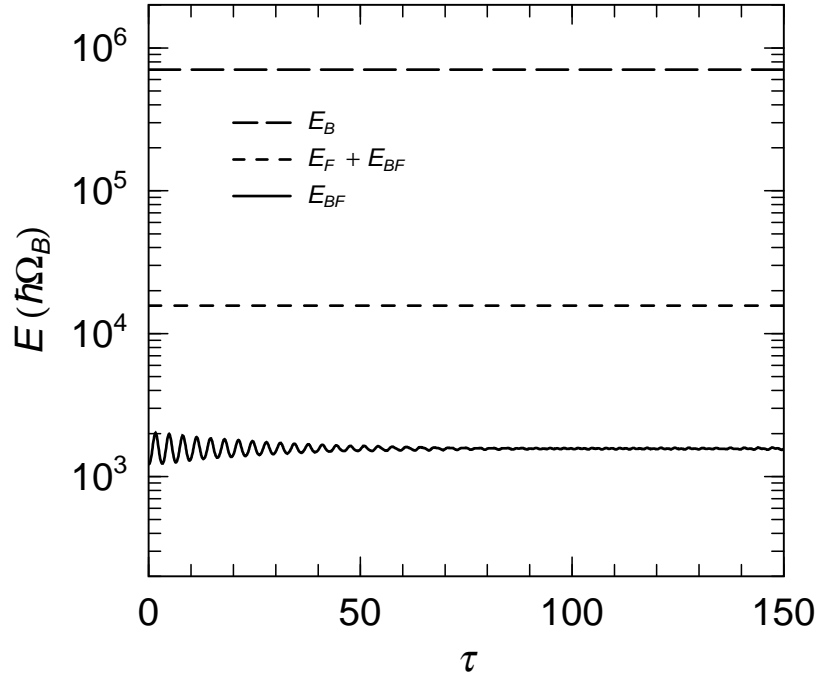


FIG. 5: Time evolution of the boson energy part E_B , the fermion energy E_F and the boson-fermion interaction energy E_{BF} . Same as Fig. 4

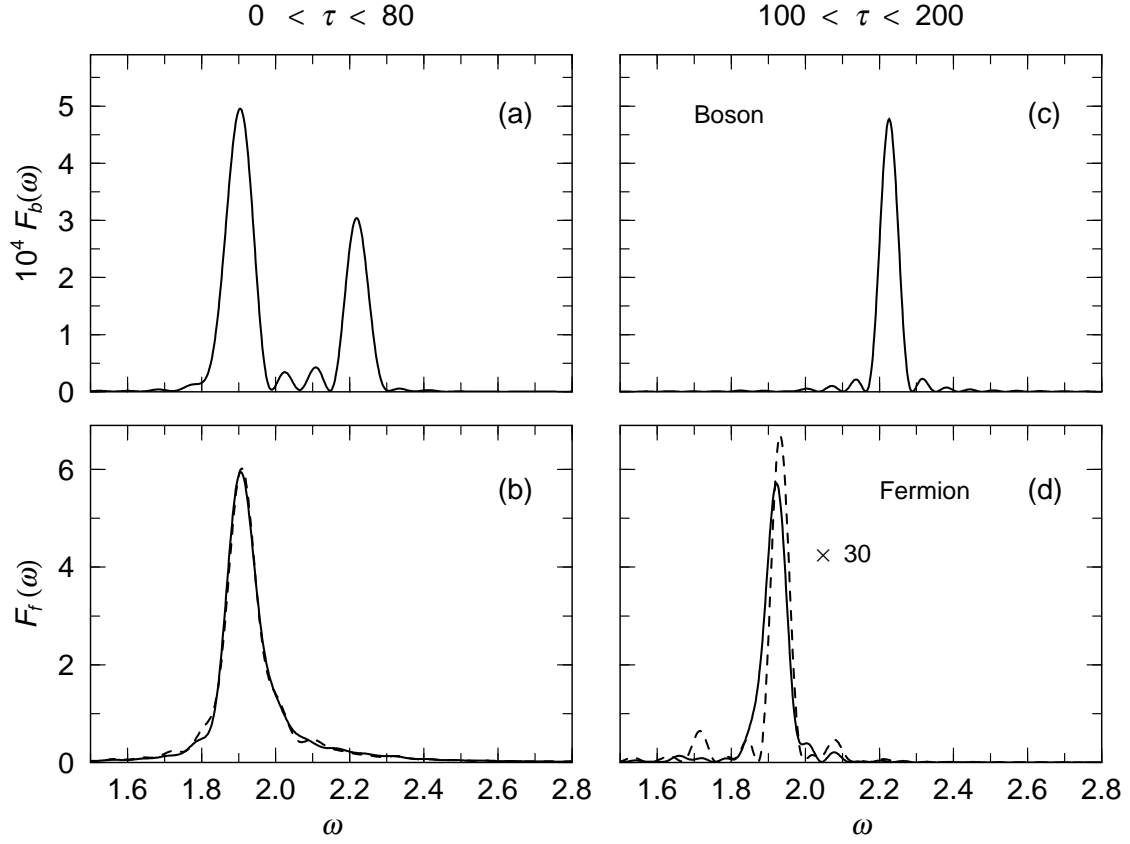


FIG. 6: Spectra of the boson oscillation in upper columns (a,c,e) and fermion oscillation in down columns (b,d,f). The spectra deduced from the evolution in $0 < \tau < 30$ are shown in the left columns, that in $30 < \tau < 60$ are in the central columns and that in $100 < \tau < 400$ are in the right columns. The frequency ω is in unit of ω_B . See Fig. 3 for the details of the oscillation.

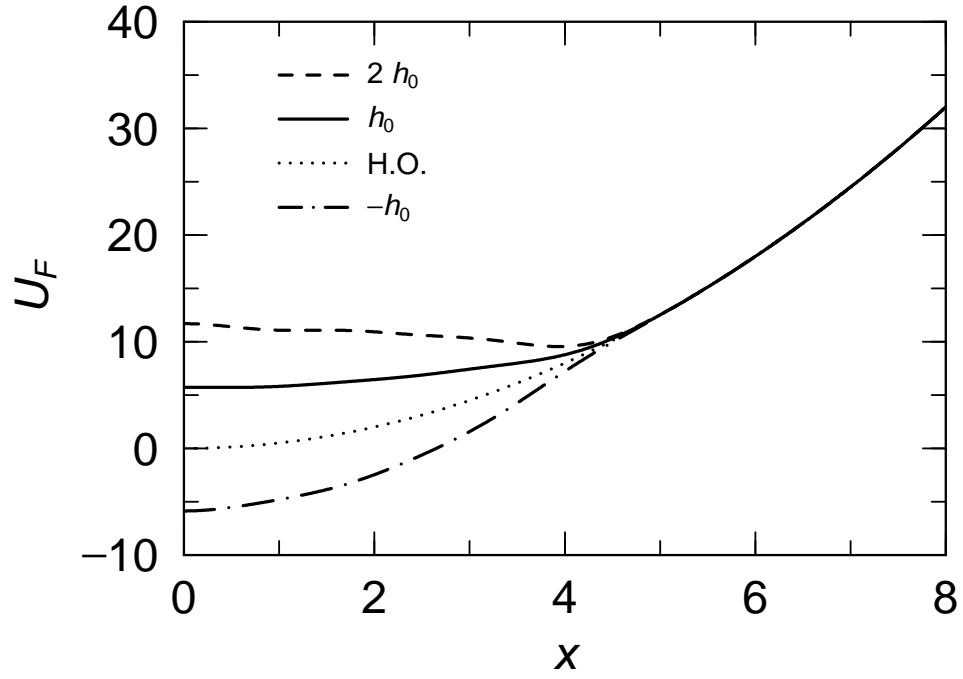


FIG. 7: Fermion potential at the ground state. The dashed, solid, and chain-dotted lines show those at $h_{BF} = 2h_0$, $h_{BF} = h_0$ and $h_{BF} = -h_0$, respectively. The dotted line indicates the harmonic oscillator potential.

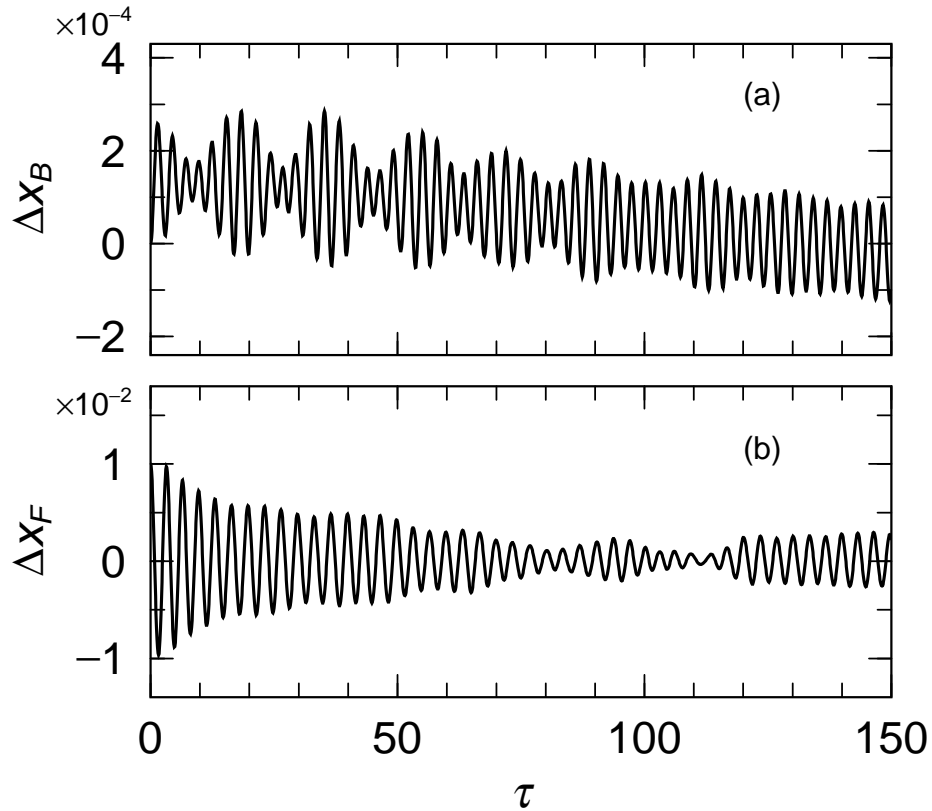


FIG. 8: Time evolution of x for boson (a) and fermion (b) with $h_{BF} = h_0$ at the initial condition that $x_B(0) = 0$ and $x_F(0) = 0.01$.

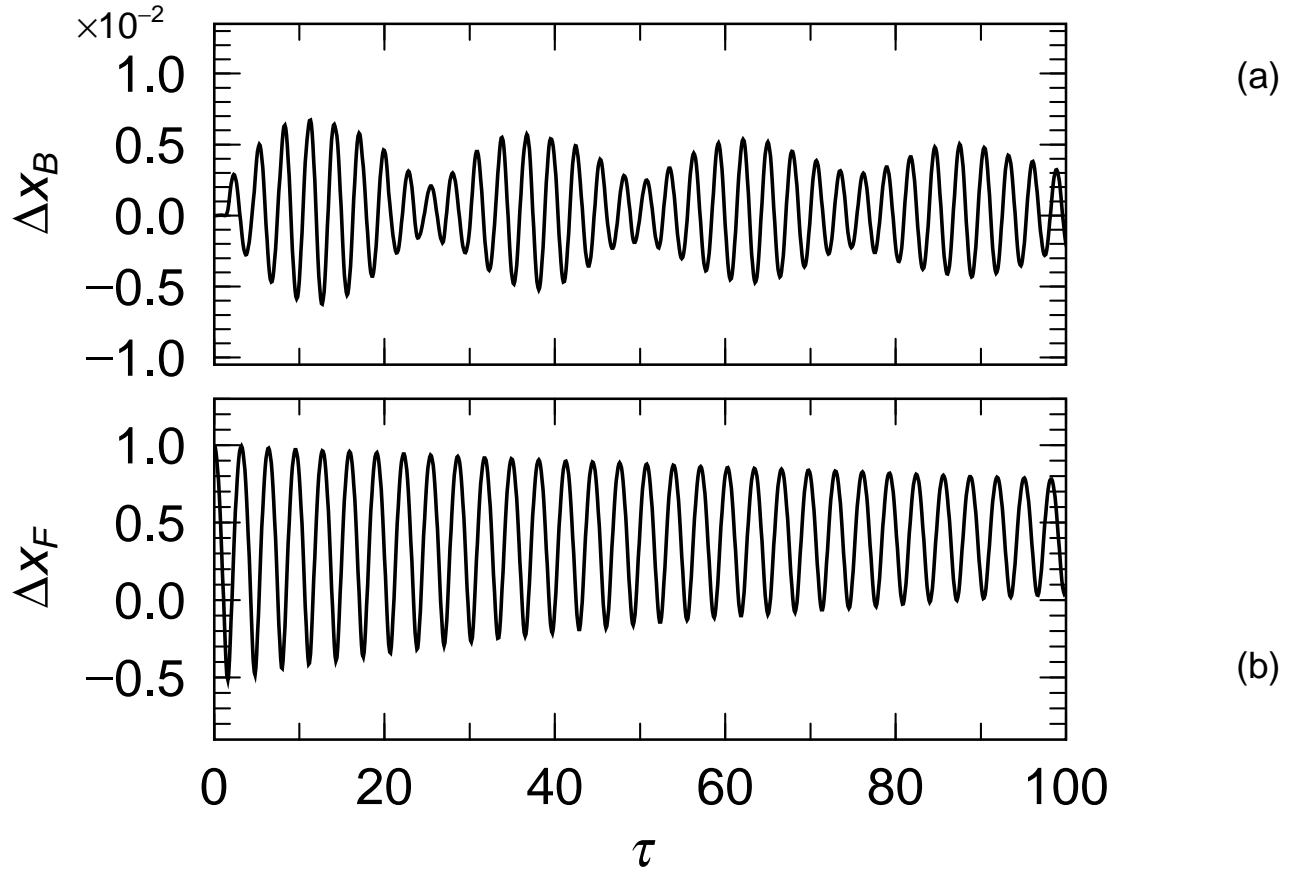


FIG. 9: Time evolution of x for boson (a) and fermion (b) with $h_{BF} = h_0$ at the initial condition that $x_B(0) = 0$ and $x_F(0) = 1.0$.

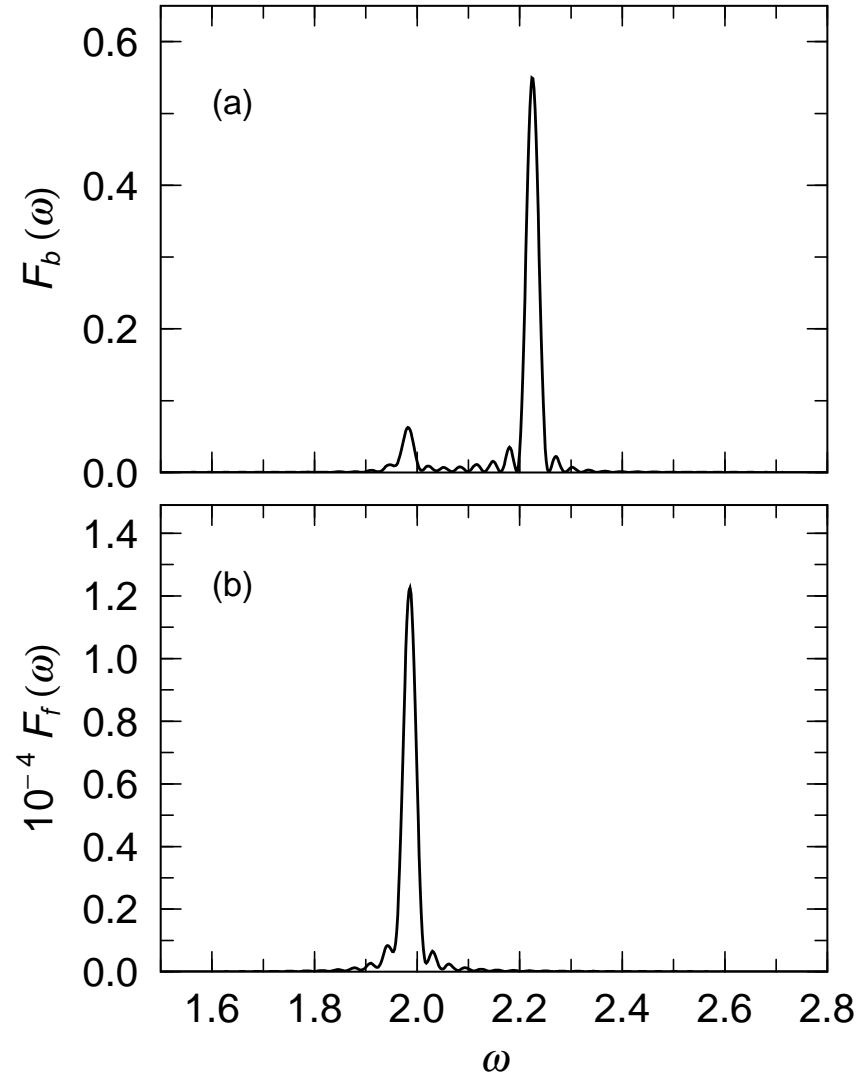


FIG. 10: Spectra of the boson oscillation in upper columns (a) and fermion oscillation (b) at the initial condition that $x_B(0) = 0$ and $x_F(0) = 1.0$. The spectra are deduced from the evolution in $0 < \tau < 200$ in the oscillation shown in Fig. 9.

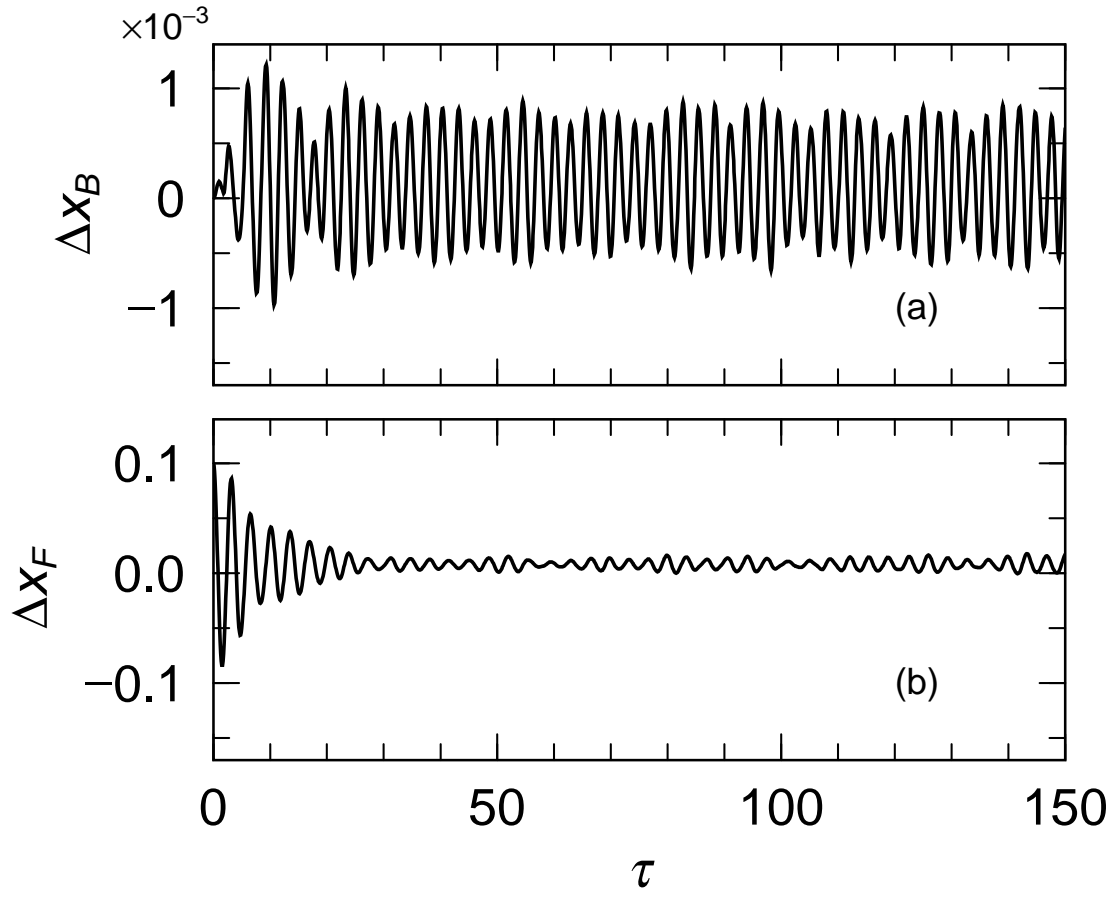


FIG. 11: Time evolution of x for boson (a) and fermion (b) at the initial condition that $x_B(0) = 0$ and $x_F(0) = 0.1$ with the boson-fermion coupling $h_{BF} = 2h_0$

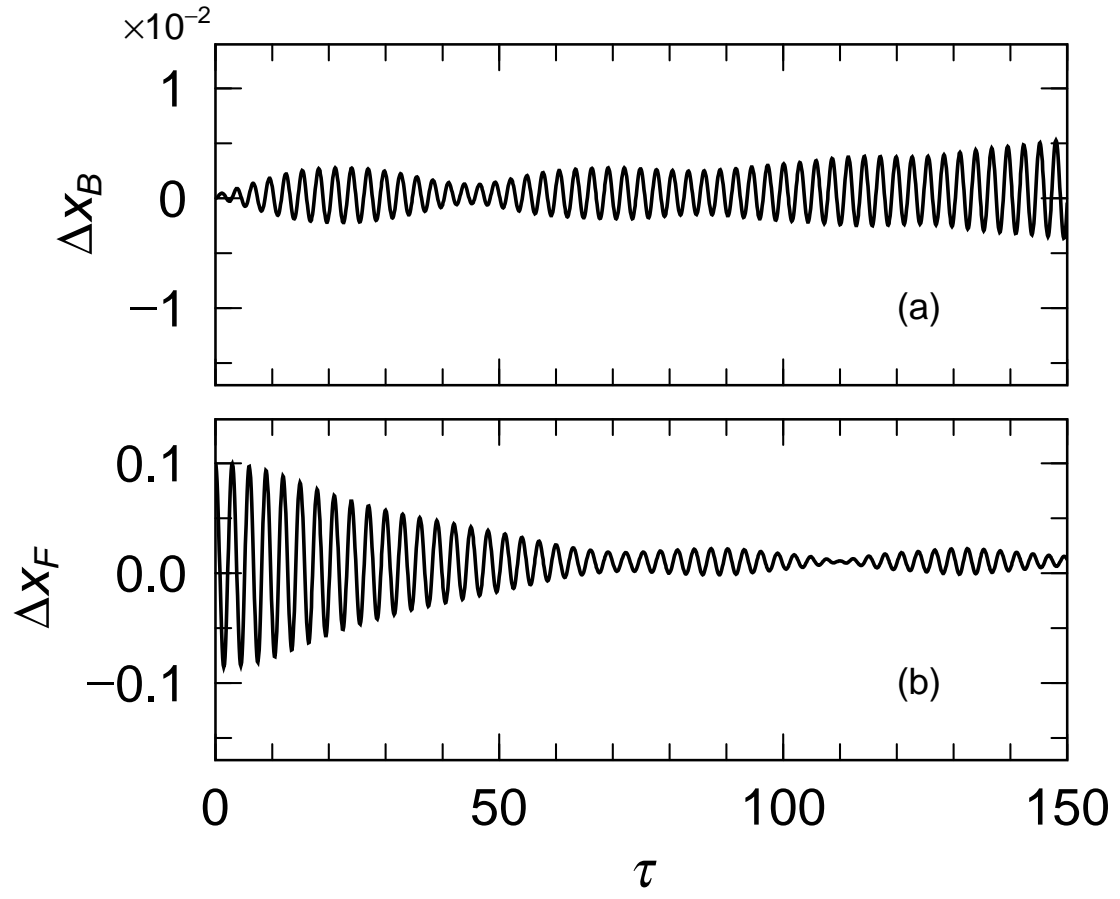


FIG. 12: Time evolution of x for boson (a) and fermion (b) at the initial condition that $x_B(0) = 0$ and $x_F(0) = 0.1$ with the boson-fermion coupling $h_{BF} = h_0$